Research Article

Rosalba Moretta, Monica Terracciano*, Principia Dardano, Maurizio Casalino, Ilaria Rea, and Luca De Stefano

Covalent grafting of graphene oxide on functionalized macroporous silicon

https://doi.org/10.1515/oms-2018-0002
Received Aug 04, 2017; revised Oct 05, 2017; accepted Oct 07, 2017

Abstract: Graphene oxide (GO) is a single-atom-thick and two-dimensional carbon material that has attracted great attention because of its remarkable electronic, mechanical, chemical and thermal properties. GO could be an ideal substrate for the development of label-free optical biosensors, however, its weak photoluminescence (PL) strongly limits the use for this purpose. In this study, we developed a covalent chemical strategy in order to obtain a hybrid GO-macroporous silicon (PSi) structure for biomedical applications. The realized structure was characterized by atomic force microscopy (AFM), scanning electron microscopy (SEM) water contact angle (WCA) measurements, Fourier transform infrared spectroscopy (FTIR) and label–free optical methods based on spectroscopic reflectometry and PL analysis. Investigations showed that the hybrid structure is suitable as a transducer material for biosensing applications due to its peculiar optical properties resulting from the combination of GO and PSi.

Keywords: porous silicon, graphene oxide, surface functionalization, interferometry, photoluminescence

1 Introduction

Graphene oxide (GO) is one-atom-thick planar sheet of sp^2-bonded carbon atoms, arranged in a hexagonal pattern like a two-dimensional honeycomb lattice [1, 2]. GO exhibits innovative mechanical, thermal, electrical and optical properties which make this two-dimensional (2D) material attracting and under continuous research [3–5]. It also displays favourable characteristics owing to the heterogeneous chemical and electronic structure; the possibility of being processed in solution and chemically tuned; the hydrophilic nature due to the oxygen containing functional groups (*i.e.*, carboxyl, epoxy and hydroxyl groups) which provide great water dispersibility and biocompatibility. These properties of GO have provided a lot of opportunities for the development of novel biosensing systems [5–11]. Moreover, the discovery of the steady-state photoluminescence (PL) properties of GO, PL emission from 500 to 800 nm reported on exposure to near UV radiation, has opened new perspectives in optoelectronics [12]. Unfortunately, the PL of GO is very weak due oxygen functional groups producing non-radiative recombination as a result of transfer of their electrons to the holes present in sp^2 clusters [13]. A common way to enhance GO light generation is based on reduction or oxidation treatments [14, 15]. A recent approach to increase PL emission from GO is the infiltration of this material into large specific surface area substrates such as porous silicon (PSi) [16]. PSi, obtained by electrochemical partial dissolution of doped crystalline silicon, due to its high specific surface area, optical and electrical properties, tailorable morphology and surface chemistry is one of the most intriguing optical transducer for developing of a wide range of chemical and biological sensors [17, 18]. In our recent papers, we reported the formation of GO-PSi hybrid systems based on electrostatic interaction between GO nanosheets and amino-modified mesoporous silicon. The GO nanosheets were infiltrated by spin-coating into different silanized PSi structures: a homogeneous monolayer and an aperiodic multilayer Thue-Morse formed by 64 layers [19, 20]. Both hybrid structures showed an intense PL signal on a broad range of optical frequencies and enhancement of the PL emitted from GO by several factors with respect to GO deposited on crystalline silicon, without losing sensing abilities. In biosensor development, a covalent bound of functional components onto transducer surfaces is advanta-

***Corresponding Author: Monica Terracciano:** Institute for Microelectronics and Microsystems, Unit of Naples, Via P. Castellino 111, 80131, Napoli, Italy; Email: monica.terracciano@na.imm.cnr.it
Rosalba Moretta: Institute for Microelectronics and Microsystems, Unit of Naples, Via P. Castellino 111, 80131, Napoli, Italy; Department of Chemical Sciences "Federico II" University of Naples, Via Cynthia, 80126 Naples Italy
Principia Dardano, Maurizio Casalino, Ilaria Rea, Luca De Stefano: Institute for Microelectronics and Microsystems, Unit of Naples, Via P. Castellino 111, 80131, Napoli, Italy

geous, in order to avoid their untimely detachment and device impairment. In this work, GO was covalently immobilized on a PEG-modified macroporous silicon layer *via* EDC/NHS chemistry. The formation of the hybrid GO-PSi was investigated by atomic force microscopy (AFM), scanning electron microscopy (SEM), water contact angle (WCA) measurements, Fourier transform infrared spectroscopy (FTIR), spectroscopic reflectometry and steady-state photoluminescence (PL). The results highlighted the presence of GO covalently bound to the surface of PSi, suggesting the possibility to use this natural photoluminescent hybrid material as platform for label-free biosensing.

2 Materials and Methods

2.1 Chemicals

Hydrofluoric acid (HF), undecylenic acid (UDA), N-(3-Dimethylaminopropyl)-N'-ethylcarbodiimide hydrochloride(EDC), N-hydroxysuccinimide (NHS), MES hydrate, tert-Butyloxycarbonyl-NH-PEG- Amine (BOC-NH-PEG-NH_2), trifluoroacetic acid (TFA), chloroform, tetrahydrofuran were purchased from Sigma Aldrich (St. Louis, MO, USA). Graphene oxide (GO) nanosheets were purchased from Biotool.com (Houston, TX, USA) as a batch of 2 mg/mL in water with a nominal sheets size included between 50 and 200 nm.

2.2 Porous silicon (PSi) fabrication and hydrosilylation process

Macroporous silicon structure was fabricated by electrochemical etching of n-type crystalline silicon (0.01-0.02 Ω cm resistivity, ⟨100⟩ oriented and 500 µm thick) in hydrofluoric acid (HF, 5% in weight)/ethanol solution at room temperature (RT). A single layer of PSi with 61% in porosity (n_{PSi} = 1.83 at λ=1.2 µm) and thickness L, of 2.1 µm and pore dimensions included between 50 and 250 nm, was obtained applying a current density of 20 mA cm^{-2} for 90 s [21]. Before the etching procedure, the silicon substrate was immersed in HF solution for 2 min to remove the native oxide layer. As-etched PSi device was placed in a Schlenk tube containing deoxygenated neat UDA (99% v/v) and allowed to react at 110°C for 18 h under a stream of argon. Afterwards, the PSi structure was extensively washed in tetrahydrofuran and chloroform so as to remove excess unreacted reagent [22].

2.3 PSi PEGylation and covalent grafting of graphene oxide

The PEGylation of PSi was carried out by immersing the structure in BOC-NH-PEG-NH_2 solution (0.4 M, overnight, at 4°C.) by using EDC/NHS (0.005 M, in MES 0.1 M, 90 min, at RT) [23, 24]. In order to remove excess reagents, the sample was rinsed in MES buffer and deionized water. A solution of TFA (95% v/v, 90 min, at RT) was used to remove the BOC protective group from the second amine portion of PEG molecule, covalently bond to PSi-surface. The excess of TFA was removed by rinsing the sample in deionized water. The GO solution was sonicated for 3 hours and left to decant for 2 days; the supernatant was separated from precipitate and used for the experiment [20]. Finally, GO (1 mg/mL) was covalently conjugated to PEGylated PSi by using EDC/NHS solution (0.005M, in MES 0.1 M, overnight at RT).

2.4 Atomic Force Microscopy

A XE-100 AFM (Park Systems) was used for the imaging of PSi substrate before and after functionalization with GO. Surface imaging was obtained in noncontact mode using silicon/aluminum coated cantilevers (PPP-NCHR 10M; Park Systems) 125 µm long with resonance frequency of 200 to 400 kHz and nominal force constant of 42 N/m. The scan frequency was typically 1 Hz per line.

2.5 Scanning Electron Microscopy

SEM images have been performed at 5kV accelerating voltage and 30 µm wide aperture by a Field Emission Scanning Electron Microscope (Carl Zeiss NTS GmbH 1500 Raith FE-SEM). A InLens detector has been used. A section of the samples has been tilted at 90° in order to perform SEM analysis in lateral view.

2.6 Water contact angle measurements

Sessile drop technique has been used for water contact angle (WCA) measurements on a First Ten Angstroms FTA 1000 C Class coupled with drop shape analysis software. The WCA values reported in this work are the average of at least three measurements on the same sample.

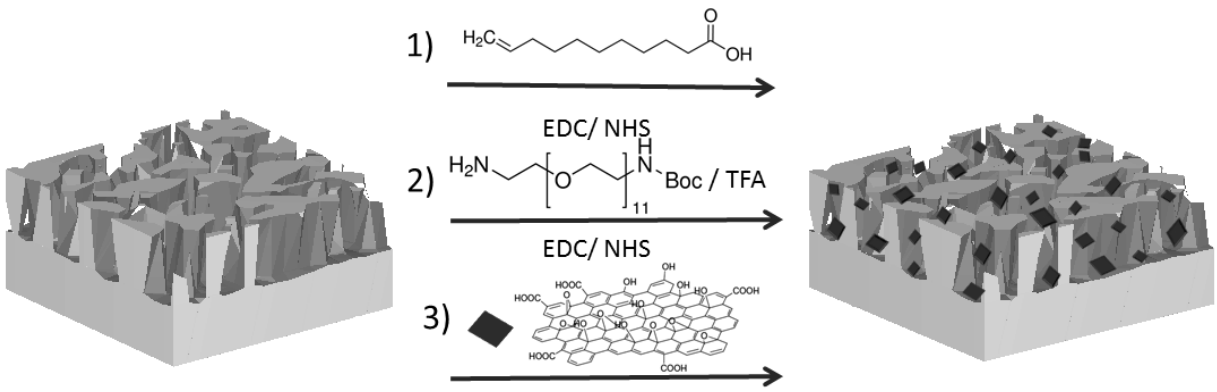

Scheme 1: Schematic representation of the PSi covalent functionalization with GO. Reaction 1, the hydrosilylation process of PSi with undecylenic acid, 18 h @110°C. Reaction 2, the PEGylation of PSi via EDC/NHS (ON @RT) and selective deprotection of -NH-BOC by TFA (90 min @RT). Reaction 3, the GO conjugation of PEGylated PSi via EDC/NHS (ON @RT).

2.7 Fourier Transform Infrared Spectroscopy

The Fourier transform infrared spectra of all samples were obtained using a Nicolet Continuμm XL (Thermo Scientific) microscope in the wavenumber region of 4000-650 cm^{-1} with a resolution of 4 cm^{-1}.

2.8 Spectroscopic reflectometry

The reflectivity spectra of PSi sample were measured at normal incidence by means of a Y optical reflection probe (Avantes), connected to a white light source and to an optical spectrum analyzer (Ando, AQ6315B). The spectra were collected over the range 800-1500 nm with a resolution of 5 nm. Reflectivity spectra shown in the work are the average of three measurements.

2.9 Steady-state photoluminescence

Steady-state photoluminescence (PL) spectra were excited by a continuous wave He-Cd laser at 442 nm (KIMMON Laser System). PL was collected at normal incidence to the surface of samples through a fiber, dispersed in a spectrometer (Princeton Instruments, SpectraPro 300i), and detected using a Peltier cooled charge coupled device (CCD) camera (PIXIS 100F). A long pass filter with a nominal cut-on wavelength of 458 nm was used to remove the laser line at monochromator inlet.

3 Results and Discussion

3.1 Realization of GO-PSi structure and morphological surface characterizations

The GO structure is characterized by epoxy and hydroxyl functional groups covalently bonded on either side of a basal plane with carboxyl groups at the edge sites, resulting highly hydrophilic contrary to graphene [25, 26]. Moreover, the carboxyl groups make GO much more attractive than graphene, because they provide handles for the connection of GO sheets to different substrates (*e.g.*, polymer, nanoparticles, DNA, silicon substrates, etc) for the development of functional GO-based materials [27–29]. In order to covalently immobilize GO nanosheets on macroporous silicon, the structure was firstly hydrosilylated by undecylenic acid (Scheme 1, step 1) [22, 30]. PSi suffers from aging phenomena, with a consequent oxidation of the internal surface of the pores and a lowering in the effective refractive index of the structure, which is crucial for a photonic device [31, 32]. A develop of a valid strategy to both stabilize and functionalize PSi support is a key issue for the biosensor realization. The hydrosilylation process is a valid strategy to passivate/functionalize the PSi surface from oxidation and corrosion in aqueous solutions, as described in SI. † The thermal reaction of undecylenic acid with a hydrogen-terminated PSi induced the formation of an organic monolayer covalently attached to the surface through Si-C bonds. The carboxyl group of UDA remained intact and it could be used for a further surface functionalization [33]. In order to improve the hydrophilicity and to promote the GO grafting, the hydrosilylated-PSi (UDA-PSi) was PEGylated by BOC-NH-PEG-NH_2 via EDC/NHS and -NH-BOC deprotected by TFA (Scheme 1, step 2) [24]. Fi-

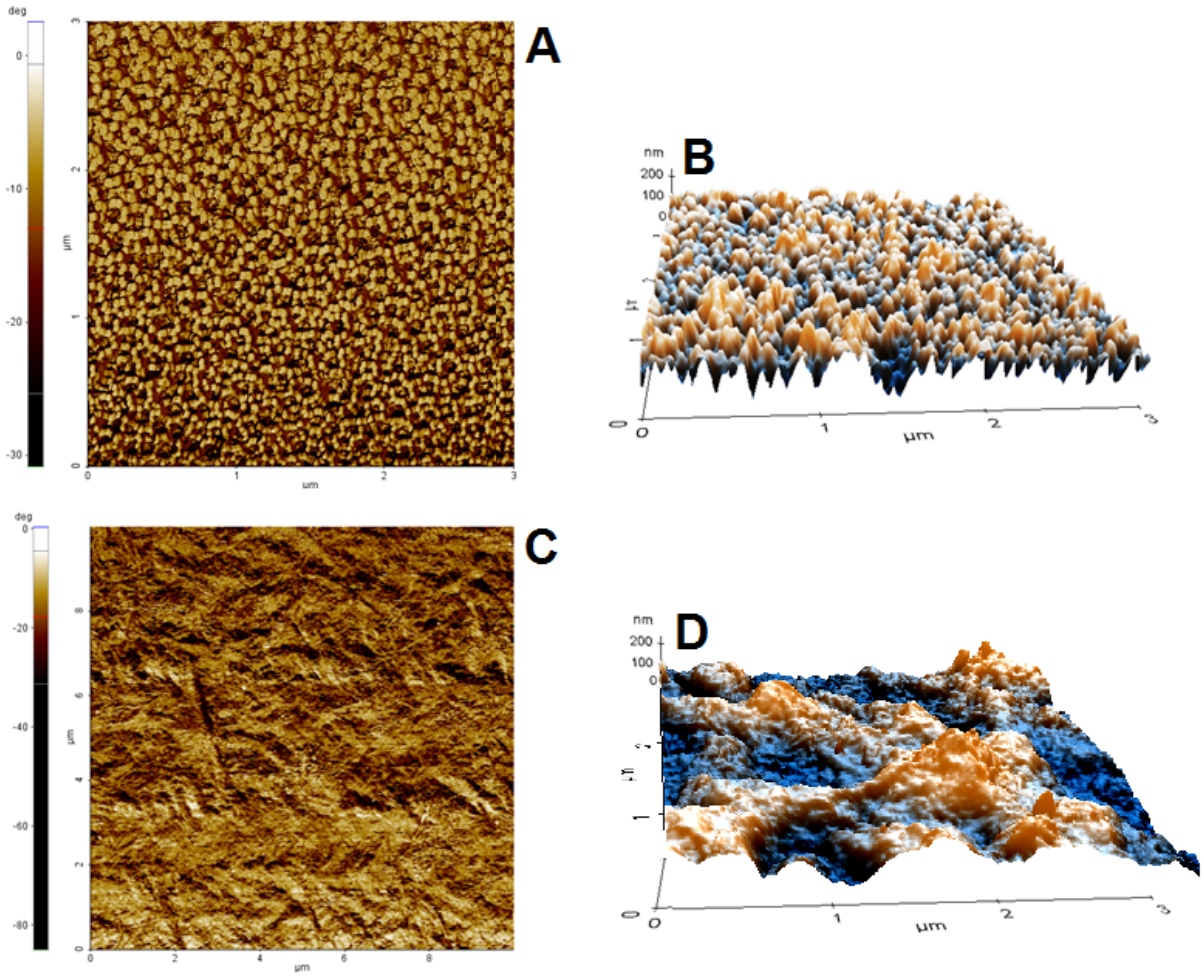

Figure 1: AFM characterization of functionalized PSi before (A: phase; B: three-dimensional rendered) and after (C: phase; D: three-dimensional rendered) GO immobilization.

nally, the GO was covalently immobilized on PEGylated-PSi (NH_2-PEG-NH-PSi) via EDC/NHS. A direct evidence of GO-grafting PSi is the evaluation of PSi morphology by AFM characterization. The AFM images of bare PSi, and GO-modified PSi surfaces are reported in Figure 1. AFM image of PSi reveals a sponge-like structure characterized by hillocks and voids distributed on the whole surface (Figure 1, A; B). After GO grafting (Figure 1, C; D), most voids disappear due to partial pore cloaking by GO nanosheets [34]. The top view SEM images in Figure 2 show the perfect coverage of the PSi substrate (bare PSi in top side) by GO flakes. Moreover, as shows in the lateral view of the tilted section of the GO-PSi compound, GO penetrates into the PSi channels

3.2 Assessment of PSi surface wettability and FTIR analysis

The control of surface wettability plays a key role in the development of hybrid interfaces [35, 36]. The variation of surface wettability after each step of functionalization was evaluated by WCA measurements, as shown in Figure 3. The surface of as-etched PSi was hydrophobic, resulting in the a WCA value of 130 (1) ° (Figure 3, A). Undecylenic acid, characterized by a carboxyl terminal-alkyl chain, induced a weak decrease of WCA to 105 (1) ° (Figure 3, B). The PEGylation step of UDA-PSi with BOC-NH-PEG-NH_2 induced a further decrease of WCA to 88 (1) ° due to the hydrophilicity of PEG chain (Figure 3, C). The removal of the BOC protector group by TFA treatment and the exposure of the amine-group made the PSi surface more hydrophilic with a WCA of 49(1) ° (Figure 3, D). Finally, the conjugation of GO to PEG-modified PSi was confirmed by a further decrease

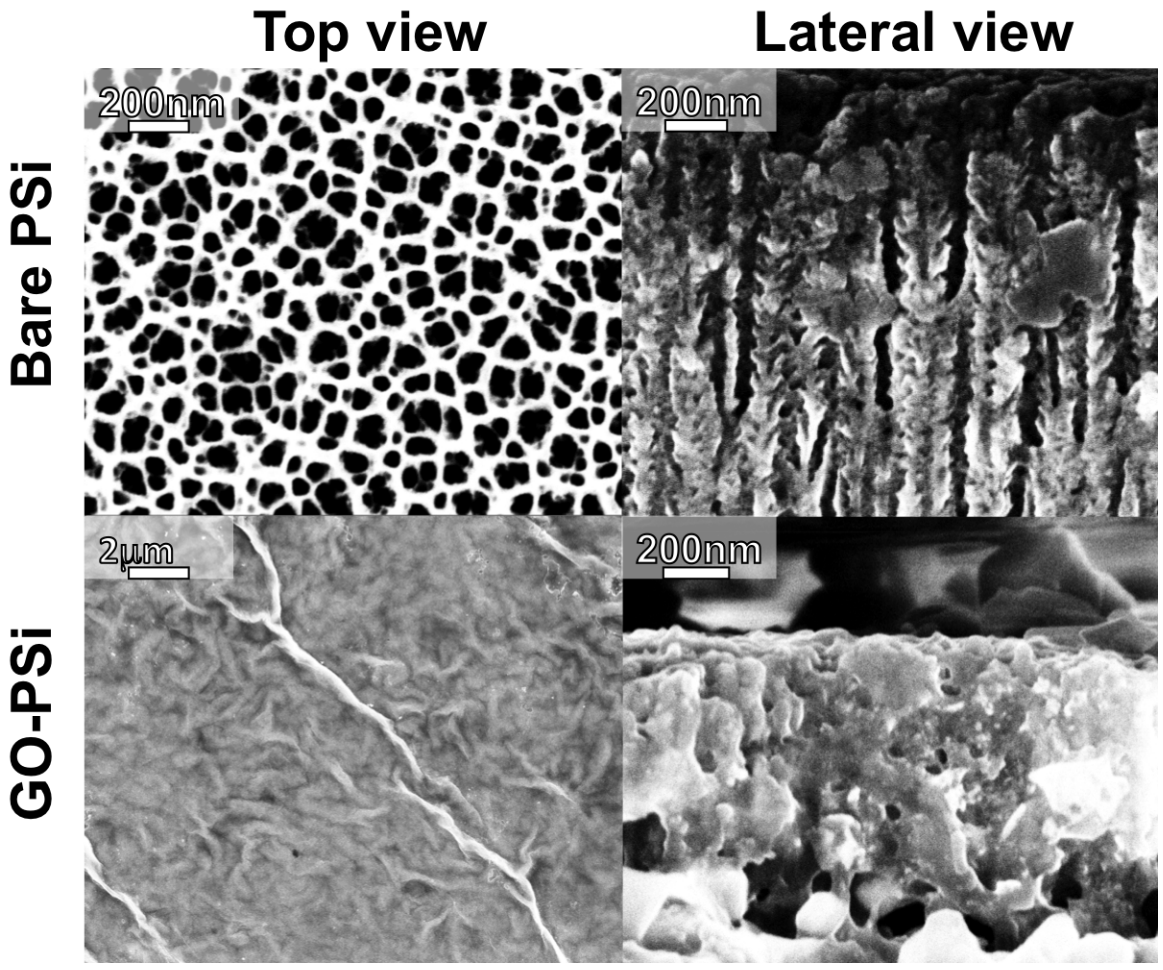

Figure 2: SEM images of bare PSi (upper images) and GO-PSi compound (lower images). Confronting both top and lateral views, the coverage and the penetration of GO into PSi substrate is confirmed by the structural characterization.

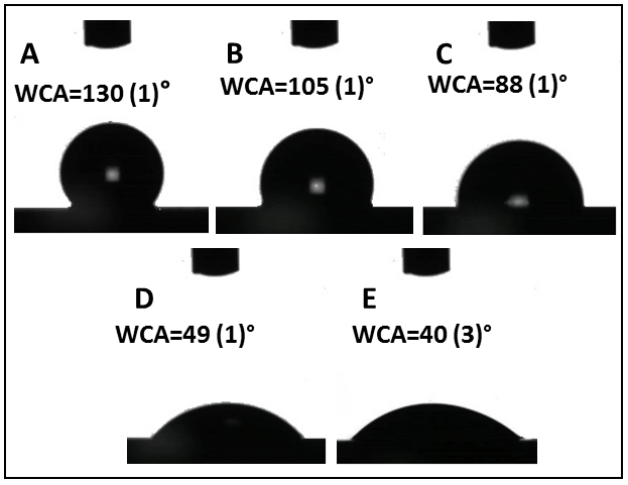

Figure 3: Water contact angle measurements performed on PSi before (A), after hydrosilylation (B), after PEGylation (C), after -NH-BOC deprotection (D) and after GO immobilization (E).

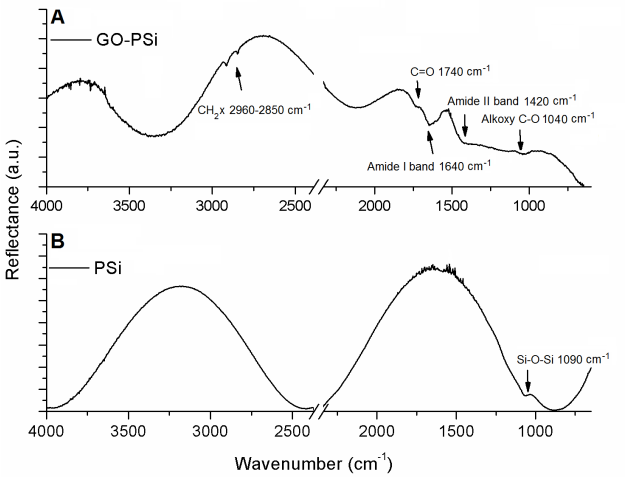

Figure 4: FTIR spectra of PSi structure before (A) and after (B) covalent grafting of GO sheets.

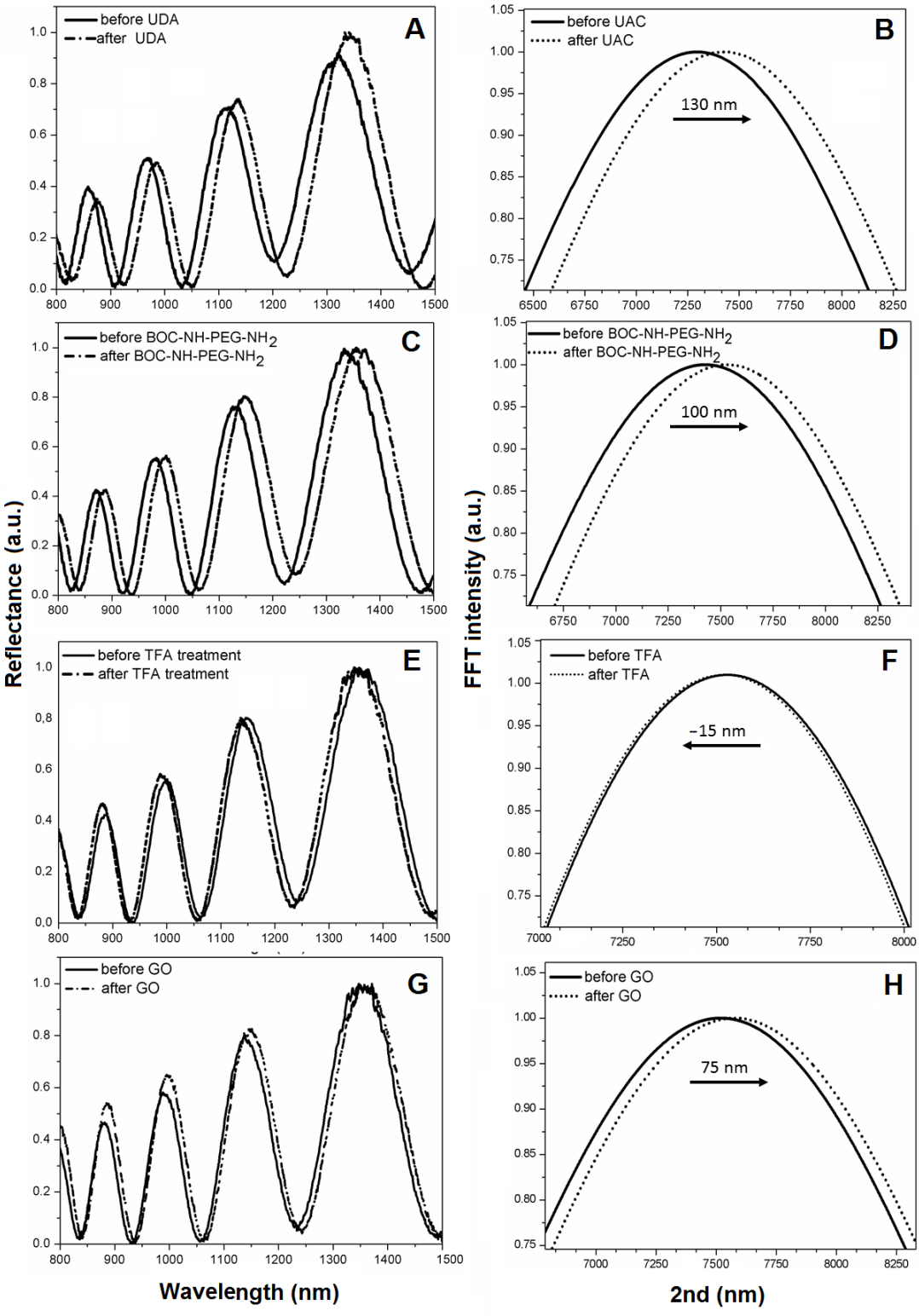

Figure 5: Reflectivity spectra (A) and corresponding Fourier transforms (B) of PSi before (solid line), and after (dashed line) UDA treatment. Reflectivity spectra (C) and corresponding Fourier transforms (D) of UDA-PSi before and after PEGylation with BOC-NH-PEG-NH_2 (dashed line). Reflectivity spectra (E) and corresponding Fourier transforms (F) of PEGylated PSi before (solid line) and after selective deprotection of -NH-BOC by TFA treatment (dashed line). Reflectivity spectra (G) and corresponding Fourier transforms (H) of deprotected PEG-PSi before (solid line) and after GO immobilization (dashed line).

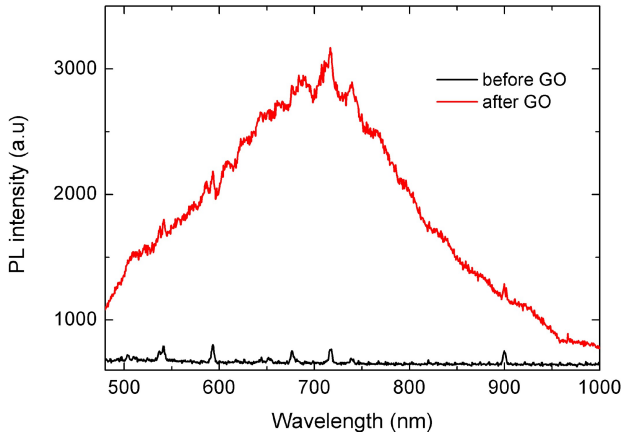

Figure 6: Photoluminescence spectra of macroporous silicon before (black line) and after GO immobilization (red line).

of WCA value to 40 (1) ° due the oxygen containing functional groups of GO (Figure 3, E). The covalent grafting of GO on PSi substrate was investigated by FTIR spectroscopy (Figure 4). FTIR spectrum of bare PSi (Figure 4, A) showed a peak of Si–O–Si stretching mode at 1090 due to spontaneous ageing of PSi during the handling [22]. After the grafting of GO the PSi structure displayed characteristic bands of GO corresponding to the CH_x at 2960-2850 cm^{-1} of carbon networks, the C=O carbonyl stretching of –COOH at 1740 cm^{-1} and the alkoxy C–O at 1040 cm^{-1} [37]. Moreover, the GO-PSi spectrum showed peaks at 1640 cm^{-1} and 1420 cm^{-1} of amide band I and II of peptide bond, respectively, confirming the covalent immobilization of GO on PSi (Figure 4, B) [38].

3.3 Characterization of PSi reflectivity and PL spectra

The optical thickness (*i.e.*, OT) of the obtained GO-PSi device was calculated from the reflectivity spectrum by FFT, which displayed a peak whose position along the x-axis corresponded to two times the optical thickness (2OT) of the layer [19]. Normal incidence reflectivity spectra of PSi before and after hydrosilylation with UDA and after the PEGylation are shown in Figure 5 (A; C) together with the corresponding FFTs (Figure 5, B; D). Since the physical thickness d of the PSi layer was fixed, the FFT peak shift of about 130 nm after UDA treatment and 100 nm after the PEGylation, due to an increase of the average refractive index (n) [21]. Figure 5 shows reflectivity spectra (E; G) with corresponding FFTs (F; H) of PEGylated PSi before and after the deprotection of –NH-BOC and after the immobilization of GO. A calculated FFT peak shift of -15 nm after TFA treatment, confirms the removal of BOC protector group from $-NH_2$. A FFT peak shift of 75 nm after the treatment of PSi with GO, confirms the successful of the GO covalent immobilization on PSi. The presence of GO on the surface of macroporous silicon was also confirmed by PL measurements. Light emission from PSi functionalized with GO nanosheets was investigated at an excitation wavelength of 442 nm. PL spectra of PSi before (black line) and after (red line) GO modification are reported in Figure 6. Any PL signal cannot be detected in the case of bare PSi. Otherwise, after GO immobilization, a strong emission in the range included between 500 and 900 nm with a maximum at about 720 nm was experimentally measured. This PL signal was attributed to the GO nanosheets covalently bond to PSi surface.

4 Conclusions

In summary, in this work we demonstrated the realization of a hybrid GO-PSi device and investigated its properties for application in biosensing. In order to develop a biosensor based on GO-PSi, the PSi structure was passivated by a UDA compound, functionalized by PEG molecules which improved the surface hydrophilicity and provided coupling points to immobilize GO via EDC/NHS chemistry. The device functionalization was confirmed qualitatively and quantitatively by several complementary techniques, such as AFM and SEM microscopy, WCA measurements, FTIR analysis and label–free optical methods based on spectroscopic reflectometry followed by FFT and PL analysis. The GO-PSi hybrid device, obtained by a covalent chemistry approach, can be used as transducer material for a wide range of applications, from biomedical diagnostics and environmental monitoring to food quality control.

References

[1] Zhu, Y., Murali, S., Cai, W., Li, X., Suk, J. W., Potts, J. R., et al., Graphene and graphene oxide: synthesis, properties, and applications. Advanced Materials 22, 2010, 3906–3924.

[2] Dreyer, D. R., Park, S., Bielawski, C. W. , and Ruoff, R. S., The chemistry of graphene oxide. Chemical Society Reviews 39, 2010, 228–240.

[3] Park, S. and Ruoff, R. S., Chemical methods for the production of graphenes. Nature Nanotechnology 4, 2009, 217–224.

[4] Compton, O. C. and Nguyen, S. T., Graphene oxide, highly reduced graphene oxide, and graphene: versatile building blocks for carbon-based materials. Small 6, 2010, 711–723.

[5] Loh, K. P., Bao, Q., Eda, G., and Chhowalla, M., Graphene oxide as a chemically tunable platform for optical applications. Nature

Chemistry 2, 2010, 1015–1024.
[6] Hunt, A., Dikin, D. A., Kurmaev, E. Z., Boyko, T. D., Bazylewski, P., Chang, G. S., et al., Epoxide speciation and functional group distribution in graphene oxide paper-like materials. Advanced Functional Materials 22, 2012, 3950–3957.
[7] Gao, W., Alemany, L. B., Ci, L., and Ajayan, P. M., New insights into the structure and reduction of graphite oxide. Nature Chemistry 1, 2009, 403–408.
[8] Liu, Y., Dong, X., and Chen, P., Biological and chemical sensors based on graphene materials. Chemical Society Reviews 41, 2012, 2283–2307.
[9] Zhang, Y., Wu, C., Guo, S., and Zhang, J., Interactions of graphene and graphene oxide with proteins and peptides. Nanotechnoly Reviews 2, 2013, 27–45.
[10] Wang, Y., Li, Z., Wang, J., Li, J. and Lin, Y., Graphene and graphene oxide: biofunctionalization and applications in biotechnology. Trends in Biotechnology 29, 2011, 205–212.
[11] Chung, C., Kim, Y. K., Shin, D., Ryoo, S. R., Hong, B. H., and Min, D. H., Biomedical applications of graphene and graphene oxide. Accounts of Chemical Research 46, 2013, 2211–2224.
[12] Chien, C. T., Li, S. S., Lai, W. J., Yeh, Y. C., Chen, H. A., Chen, I. S., et al., Tunable photoluminescence from graphene oxide, Angewandte Chemie International Edition 51, 2012, 6662–6666.
[13] Gupta, A., Shaw, B. K., and Saha, S. K., Bright green photoluminescence in aminoazobenzene-functionalized graphene oxide. The Journal of Physical Chemistry C 118, 2014, 6972–6979.
[14] Eda, G., Lin, Y. Y., Mattevi, C., Yamaguchi, H., Chen, H. A., Chen, I. S., Blue photoluminescence from chemically derived graphene oxide. Advanced Materials 22, 2010, 505–509.
[15] Gokus, T., Nair, R. R., Bonetti, A., Lombardo, A., Novoselov, K. S., Geim, A. K., et al., Making Graphene Luminescent by Oxygen Plasma Treatment. ACS Nano 3, 2009, 3963–3968.
[16] Hummers, W. S. and Offeman, R. E., Preparation of graphitic oxide. Journal of the American Chemical Society 80, 1958, 1339–1339.
[17] Canham, L., Properties of porous silicon. Institution of Electrical Engineers, 1997.
[18] Sailor, M. J., Porous silicon in practice: preparation, characterization and applications. Wiley-VCH, 2012.
[19] Rea, I., Sansone, L., Terracciano, M., De Stefano, L., Dardano, P., Giordano, et al., Photoluminescence of graphene oxide infiltrated into mesoporous silicon. The Journal of Physical Chemistry C 118, 2014, 27301–27307.
[20] Rea, I., Casalino, M., Terracciano, M., Sansone, L., Politi, J. and De Stefano, L., Photoluminescence enhancement of graphene oxide emission by infiltration in an aperiodic porous silicon multilayer. Optics Express 24, 2016, 24413–24421.
[21] Terracciano, M., De Stefano, L., Borbone, N., Politi, J., Oliviero, G., Nici, F., et al., Solid phase synthesis of a thrombin binding aptamer on macroporous silica for label free optical quantification of thrombin. RSC Advances 6, 2016, 86762–86769.
[22] Shabir, Q., Webb, K., Nadarassan, D. K., Loni, A., Canham, L. T., Terracciano, M., et al., Quantification and reduction of the residual chemical reactivity of passivated biodegradable porous silicon for drug delivery applications. Silicon, 2017, 1–11.
[23] Sam, S., Touahir, L., Salvador Andresa, J., Allongue, P., Chazalviel, J. N., Gourget-Laemmel, A. C., et al., Semiquantitative study of the EDC/NHS activation of acid aerminal groups at modified porous silicon surfaces. Langmuir 26, 2010, 809–814.
[24] Harris, J. M., Poly(Ethylene Glycol) Chemistry. Springer US, 1992.
[25] Dikin, D. A., Stankovich, S., Zimney, E. J., Piner, R. D., Dommett, G. H. B., Evmenenko, G., et al., Preparation and characterization of graphene oxide paper. Nature 448, 2007, 457-460.
[26] Loh, K. P., Bao, Q., Ang, P. K., and Yang, J., The chemistry of graphene. Journal of Materials Chemistry 20, 2010, 2277.
[27] Kong, L. B., Carbon nanomaterials based on graphene nanosheets, CRC Press, 2017.
[28] Yang, X., Zhang, X., Ma, Y., Huang, Y., Wang, Y., and Chen, Y., Superparamagnetic graphene oxide–Fe_3O_4 nanoparticles hybrid for controlled targeted drug carriers. Journal of Materials Chemistry 19, 2009, 2710.
[29] Lee, S. H., Dreyer, D. R., An, J., Velamakanni, A., Piner, R. D., Park, S., et al., Polymer brushes via controlled, surface-initiated atom transfer radical polymerization (atrp) from graphene oxide. Macromolecular Rapid Communications 31, 2010, 281–288.
[30] Jalkanen, T., Mäkilä, E., Sakka, T., Salonen, J., and Ogata, Y. H., Thermally promoted addition of undecylenic acid on thermally hydrocarbonized porous silicon optical reflectors. Nanoscale Research Letters 7, 2012, 311.
[31] Ghulinyan, M., Gelloz, B., Ohta, T., Pavesi, L., Lockwood, D. J., and Koshida, N., Stabilized porous silicon optical superlattices with controlled surface passivation. Applied Physics Letters 93, 2008, 61113.
[32] De Stefano, L., Oliviero, G., Amato, J., Borbone, N., Piccialli, G., Mayol, L., et al., Aminosilane functionalizations of mesoporous oxidized silicon for oligonucleotide synthesis and detection. Journal of the Royal Society Interface, 2013, 10.
[33] Boukherroub, R., Wojtyk, J. T. C., Wayner, D. D. M., and Lockwood, D. J., Thermal hydrosilylation of undecylenic acid with porous silicon. Journal of The Electrochemical Society 59, 2002, 149.
[34] Terracciano, M., Rea, I., De Stefano, L., Rendina, I., Oliviero, G., Nici, F., et al., Synthesis of mixed-sequence oligonucleotides on mesoporous silicon: chemical strategies and material stability. Nanoscale Research Letters 9, 2014, 317.
[35] Terracciano, M., Galstyan, V., Rea, I., Casalino, M., De Stefano, L., and Sbervegleri, G., Chemical modification of TiO_2 nanotube arrays for label-free optical biosensing applications. Applied Surface Science 419, 2017, 235–240.
[36] Mittal, K. L., Contact Angle, Wettability and Adhesion, VSP, 2006.
[37] Cao, L., Li, Z., Su, K. and Cheng, B., Hydrophilic Graphene preparation from gallic acid modified graphene oxide in magnesium self-propagating high temperature synthesis process. Scientific reports 6, 2016.
[38] Socrates, G., Infrared and Raman characteristic group frequencies/tables and charts. Third ed., Wiley, Chichester, 2001.